Advances in Water Resources 128 (2019) 28–38

Contents lists available at ScienceDirect

Advances in Water Resources

journal homepage: www.elsevier.com/locate/advwatres

Linking statistical and hydrodynamic modeling for compound flood hazard assessment in tidal channels and estuaries

Hamed Moftakhari[a,b], Jochen E. Schubert[a], Amir AghaKouchak[a], Richard A. Matthew[a], Brett F. Sanders[a,*]

[a] University of California, Irvine, CA, United States
[b] The University of Alabama, United States

ARTICLE INFO

Keywords:
Coastal flood hazards
Bivariate statistical analysis
Hydrodynamic modeling
Compound flooding

ABSTRACT

A method to link bivariate statistical analysis and hydrodynamic modeling for flood hazard estimation in tidal channels and estuaries is presented and discussed for the general case where flood hazards are linked to upstream riverine discharge Q and downstream ocean level, H. Using a bivariate approach, there are many possible combinations of Q and H that jointly reflect a specific return period, T, raising questions about the best choice as boundary forcing in a hydrodynamic model. We show, first of all, how possible Q and H values depend on whether the definition of T corresponds to the probability of exceedance of "H OR Q" or "H AND Q". We also show that flood hazards defined by "OR" return periods are more conservative than "AND" return periods. Finally, we introduce a new composite water surface profile to represent the spatially distributed hazard for return period T. The composite profile synthesizes hydrodynamic model results from the "AND" hazard scenario and two scenarios based on traditional univariate analysis, a "Marginal Q" scenario and a "Marginal H" scenario.

1. Introduction

Flood risk is increasing in coastal cities around the world due to several factors including population growth, economic development, sea level rise, subsidence, land use changes and intensification of rainfall (Hallegatte et al., 2013; Hanson et al., 2011). By the year 2100, between 0.2–4.6% of global population and 0.3–9.3% of global gross domestic product may be exposed to coastal flooding if no adaptation occurs (Hinkel et al., 2014).

Management of flood risk relies on statistical and hydrodynamic modeling to delineate populations and assets exposed to flooding, anticipate and monetize the consequences of flooding, and develop cost effective and socially robust interventions including infrastructure projects, insurance programs, land use and building code policy changes and emergency preparedness and response measures (Sayers et al., 2013; Luke et al., 2018). To address risks, statistical and hydrodynamic modeling is linked to delineate spatial fields of the intensity of flooding (e.g., depth and velocity) for a set of exceedance probabilities, information which is subsequently used to estimate average annual losses based on exposed assets and their vulnerability to damage (Scawthorn et al., 2006). The linking of statistical and hydrodynamic modeling is straightforward when addressing a single hazard such as river discharge, Q. Flood risk is modeled by first performing univariate frequency analysis of annual maximum discharge to estimate extreme values $\hat{Q}_T$ for yearly return periods T (e.g., $\hat{Q}_{100}$ for 100 year return period discharge). Here, the hat notation indicates annual maximum discharge and the subscript refers to the return period. Second, hydrodynamic modeling is performed with $\hat{Q}_T$ as a boundary condition to characterize spatial fields of water surface elevation at each return period, $\eta_T(x)$, where x represents distance along the river (FEMA, 2018). However, coastal hazard assessment must account for interaction of river flooding, intense rainfall, storm surge and waves and the likelihood of a coincidence in extreme and non-extreme levels of these hazards which is also known as compounding effects (Gallien et al., 2018; Moftakhari et al., 2017). One of the most important compounding effects is the interaction of river discharge and the downstream ocean level, H, in tidal channels and estuaries. Of the world's 32 largest cities, 22 are located on estuaries (Ross, 1995), at which the interactions between Q and H play a major role in flood risk estimation (Ward et al., 2018). In the U.S. alone, 140 million people (~50% of total population) live on the coast in close proximity to an estuary (Kennish, 2004).

Fig. 1 illustrates the estuarine flood hazard problem: the objective is to estimate spatially distributed extreme water levels, $\eta_T(x)$, for return period T in a tidal channel or estuary. We assume knowledge of the system geometry (e.g., bed elevation, channel width and shape) and resistance to flow (e.g., Manning resistance coefficient). We also assume

* Corresponding author.
E-mail address: bsanders@uci.edu (B.F. Sanders).

https://doi.org/10.1016/j.advwatres.2019.04.009
Received 26 September 2018; Received in revised form 4 April 2019; Accepted 10 April 2019
Available online 12 April 2019

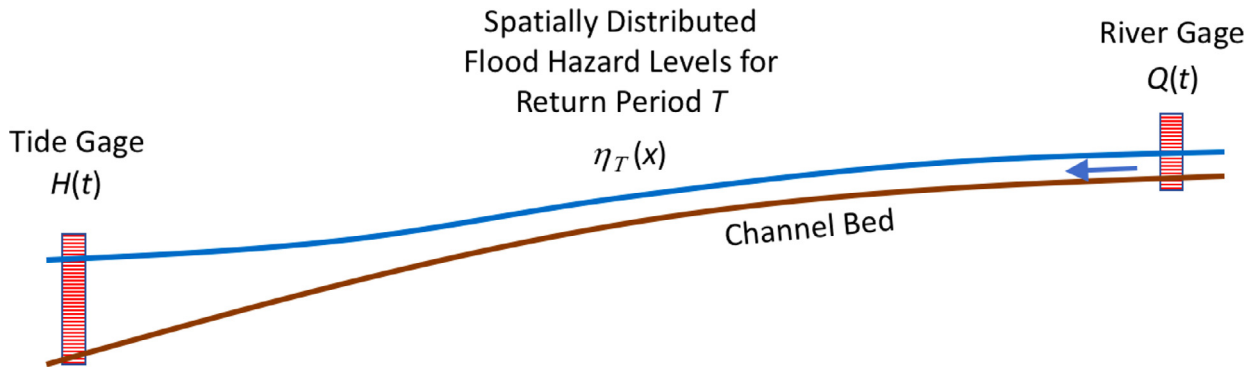

Fig. 1. The spatial distribution of the T-year return period extreme water level, $\eta_T(x)$, in an estuary or tidal channel (blue line) depends on upstream river discharge $Q(t)$, downstream ocean water levels $H(t)$, and the system geometry and resistance to flow. This paper shows how bivariate statistical analysis and hydrodynamic modeling can be linked to compute $\eta_T(x)$.

that gauges provide time series records of boundary conditions: river discharge measurements representative of what enters the reach, $Q(t)$, and water level measurements, $H(t)$, representative of the downstream end of the reach. Hence, the key question becomes: how can statistical and hydrodynamic modeling be linked for the estuarine setting involving two gage records characterizing two different aspects of hydrodynamic extremes? Put another way, can the existing paradigm of univariate flood hazard modeling described above for rivers be extended to account for a second gage in a relatively simple and straightforward way? We write this mathematically as follows,

$$\eta_T(x) = f(Q(t), H(t), p(x)) \tag{1}$$

where $p(x)$ represents the parameters describing the channel geometry and resistance properties. Note that Eq. (1) can be extended for two-dimensional flood hazard levels by interpreting x as two-dimensional vector representing geographical coordinates.

In the absence of robust models for extreme water levels in estuaries, overly simplistic bathtub models have received widespread use for estimating coastal flooding hazards and the resulting human exposure at regional (Torresan et al., 2012) and national/international levels (Dasgupta et al., 2011; Hinkel et al., 2010). Bathtub models simply take an estimated extreme water level and extrapolate it inland to estimate population and assets exposed to flooding, which neglects the potential for flood stage to change with distance inland as a consequence of riverine forcing and/or tidal damping/amplification (Lanzoni and Seminara, 1998). This points to the potential for underestimation of flood consequences. On the other hand, bathtub models may also overestimate flood consequences by failing to account for flood defenses and the role of friction, inertia and storage in flooding dynamics (Gallien et al., 2014; Sanders, 2017). By linking statistical analysis and hydrodynamic models, more robust estimates of extreme water levels become possible as well as mechanistic routing of flood water into adjacent urban areas to estimate flood impacts (Gallien et al., 2014, 2011).

Existing methods for flood hazard assessment (solving Eq. (1)) in tidal channels are limited (Hoitink and Jay, 2016). In particular, for the case where $\hat{Q}_T$ and $\hat{H}_T$ are statistically independent, FEMA (2015) recommends the following procedure to estimate the hazard for return period T: (1) univariate analysis of annual maximum river discharge to estimate $\hat{Q}_T$ and univariate analysis of annual maximum total water level to estimate $\hat{H}_T$, (2) a pair of hydrodynamic model simulations with one forced by $\hat{Q}_T$ and a non-extreme H value (usually chosen as mean higher high water) and the other forced by $\hat{H}_T$ and a non-extreme Q value, and (3) synthesis of the two hydrodynamic model simulations based on the pointwise maximum water level across the two simulations. An appealing aspect of the FEMA approach is that only two hydrodynamic simulations are required for each return period, which is important because resources for flood mapping are limited (Burby, 2001) and because hydrodynamic flood simulation is computationally demanding (i.e., many hours for one simulation) especially for urban areas where fine resolution grids are needed to accurately depict flooding, e.g., Gallien et al. (2011, 2014). Hence, the FEMA (2015) approach is aligned with needs for simple and efficient assessment approaches. Nevertheless, there are significant limitations. For example, univariate statistical analysis is not appropriate when $\hat{Q}_T$ and $\hat{H}_T$ exhibit statistical dependence also known as compound risks (Leonard et al., 2014; Moftakhari et al., 2017; Zscheischler et al., 2018). Additionally, even when $\hat{Q}_T$ and $\hat{H}_T$ are independent, extreme water levels may occur over the length of the tidal reach due to the interaction of non-extreme boundary forcing values. FEMA (2015, 2018) does not presently offer guidance to address this situation. Broadly, the FEMA (2015) guidance recommends multi-hazard assessment based on the predominant hazards, yet limitations of this approach are increasingly being recognized (Hillier et al., 2015).

The aforementioned challenges of linking statistical and hydrodynamic modeling can only be partly overcome with improved access to, and reduced costs of, high performance computing systems that map flood hazards through Monte Carlo simulation. That is, Monte Carlo simulation can be applied to depict thousands of scenarios based on different combinations of $\hat{Q}_T$ and $\hat{H}_T$, and depict spatially varied flood hazards based on the frequency of the pointwise exceedance of a water level threshold (Purvis et al., 2008). However, bivariate statistical analysis is needed in place of univariate analysis to properly describe the correlation structure of the hazard drivers and for sampling representative combinations of hazard drivers in Monte Carlo simulations.

The objective of this paper is to present a solution method for Eq. (1) that accounts for statistical correlation structure and physical compounding effects (e.g., backwater) between boundary forcing values $\hat{Q}_T$ and $\hat{H}_T$ while using only a small number of hydrodynamic model simulations. Building on the existing methodology recommended by FEMA (2015), we present a four-step method as follows:

(1) Bivariate statistical analysis of Q and H records to yield possible $(\hat{Q}_T, \hat{H}_T)$ pairs for return period, T.
(2) Selection of N specific $(\hat{Q}_T, \hat{H}_T)$ pairs for hydrodynamic modeling. Here, we recommend $N = 4$ (more detail will follow) although other options are possible.
(3) Hydrodynamic modeling of N scenarios defined by $(\hat{Q}_T, \hat{H}_T)$ pairs identified in Step 1 to yield spatial distributions of extreme water levels, $\eta_T^i(x)$, $i = 1, \ldots, N$. Note that the subscript on η references return period and the superscript references the scenario.
(4) Synthesis of hydrodynamic modeling results, $\eta_T^i(x)$, $i = 1, \ldots, N$, to yield $\eta_T(x)$.

The remainder of the paper presents this method in detail along with applications. Section 2 presents methods and materials including data used in this study, the bivariate statistical analysis methods to determine all possible $(\hat{Q}_T, \hat{H}_T)$ pairs, identification of four specific pairs useful for hydrodynamic modeling, and methods for one-dimensional steady

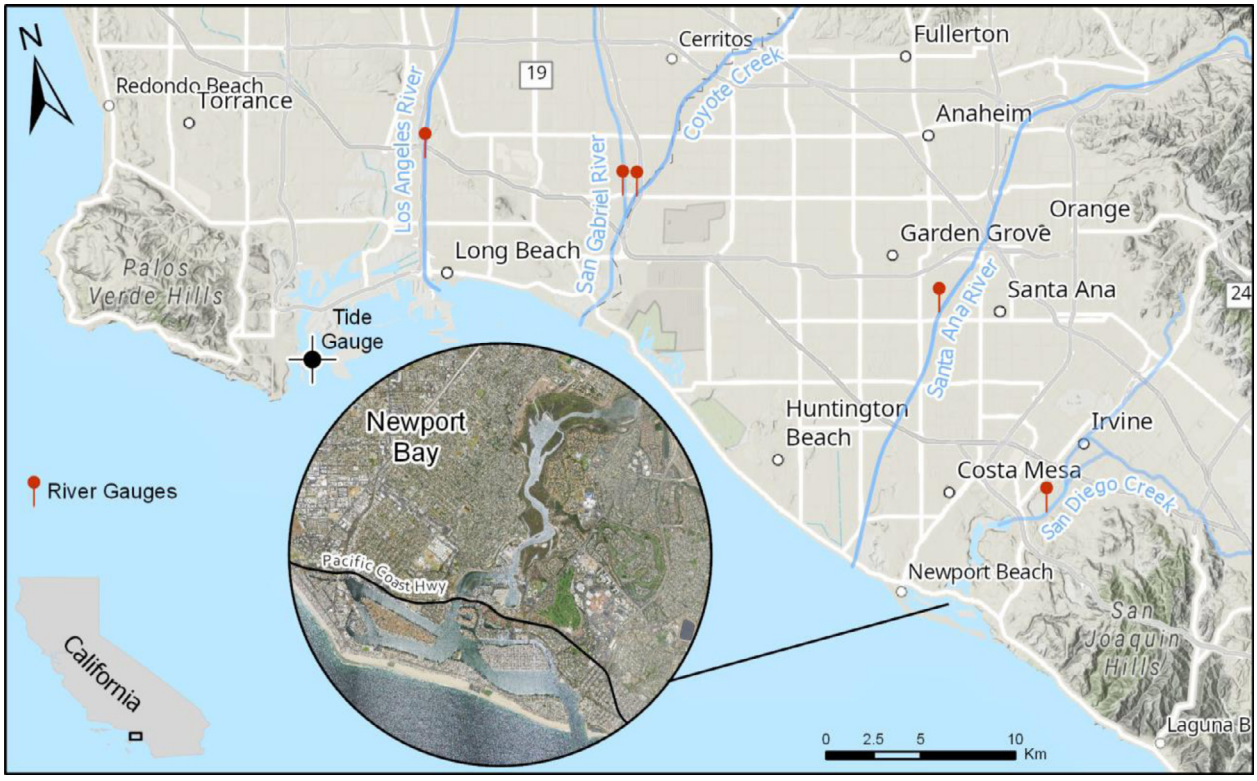

Fig. 2. Compound flood hazards in southern California were examined for Los Angeles River, San Gabriel River, Santa Ana River, and Newport Bay using river discharge and ocean water level measurements at the gage locations shown.

flow analysis and two-dimensional unsteady analysis of extreme water levels. Section 3 presents results of one-dimensional steady-flow analysis from several sites showing differences in water level profiles arising from the $(\hat{Q}_T, \hat{H}_T)$ pairs, and results of two-dimensional unsteady analysis at a single site where we further examine the limitations of the 1D modeling and the added benefits of 2D modeling for assessment of coastal flood hazards. Here, we also introduce an extension of the FEMA (2015) method that offers potential to systematically improve the assessment of coastal flood hazards by linking bivariate statistical analysis and hydrodynamic modeling. We close the paper with discussion (Section 4) and conclusions (Section 5).

Broadly, this work shows that extending the univariate paradigm of river flood hazard assessment to a bivariate paradigm of coastal flood hazard assessment is not straightforward, as has been reported for many other types of compound hazards (Kappes et al., 2012). Nevertheless, a systematic approach is possible and shown herein. Furthermore, results point to the possibility that the existing FEMA approach underestimates flood hazards where compounding effects are strong, and we present a simple method to make a better estimate.

2. Methods and materials

2.1. Data

Analysis herein focuses on tidal channels/estuaries in southern California (See Fig. 2) where flood hazards are affected by extreme ocean levels and flood discharges: the Los Angeles River (LAR), the Santa Ana River (SAR) and Newport Bay (NB). For ocean level analysis, hourly ocean water level measurements were obtained from the National Oceanic and Atmospheric Administration (NOAA) Los Angeles tide gauge (gauge ID: 9410660) at hourly intervals. Tide gauge measurements capture water level fluctuations from combined effects of tides, storm surge and other factors that affect sea levels on hourly and longer time scales, a reading that is sometimes called Total Water Level (TWL). Discharge measurements for the LAR were obtained from Los Angeles County Department of Public Works (LADPW) Station F319-R (LAR at Wardlow Road) and consisted of 92 years of annual maximum discharge data between 1928–2014. Discharge measurements for the SAR were obtained from USGS Gauge 11078000 (Santa Ana River at Santa Ana) and consisted of 94 years of annual maximum discharge data between 1923 and 2017. River discharge measurements for Newport Bay were obtained from the Orange County Department of Environmental Resources Gauge 226 (San Diego Creek at Campus Drive) and consists of 39 years of instantaneous discharge (1978–2016). The San Gabriel River and Coyote Creek (see Fig. 2) are not considered in this study since bivariate statistical analysis (see Section 3.1) showed no correlation between $\hat{Q}$ and $\hat{H}$ likely because of strong flow regulation from Whittier Narrows Dam located approximately 30 km from the coastline.

Topographic and bathymetric data for LAR, and SAR were taken from the 1 m resolution 2014 US Army Corps of Engineers National Coastal Mapping Program Topobathy Lidar DEM. Topographic and Bathymetric data for NB were based a DEM reported by Gallien et al. (2011) which merged several sources of topographic and bathymetric data.

2.2. Bivariate statistical analysis

Statistical analysis of extreme values of discharge and water level impacting a tidal reach or estuary are based on records of annual maximum values, although threshold-based approaches are also possible. Here, we use a hat notation to indicate annual maxima data from the records of upstream discharge and downstream water level, $\hat{Q}$ and $\hat{H}$, respectively. Record lengths of several decades or more are preferred to enable estimation of water levels at relatively low frequencies (e.g., return periods of 50 years or greater).

Bivariate statistical analysis begins with a test for correlation structure. While either linear or rank correlation coefficient measures can be used to assess the significance of the dependence between

variables, tail dependence measures are important for summarizing how extremes tend to occur simultaneously (Coles et al., 1999; Hao and Singh, 2016). Here, we employ joint density approaches over other alternatives (Hawkes et al., 2002; Heffernan and Tawn, 2004; Neal et al., 2013; Zheng et al., 2015) due to their flexibility, and computational/mathematical benefits (Hawkes, 2006; Salvadori et al., 2015).

According to Sklar's Theorem (Sklar, 1959), there exists a bivariate Copula function $C_{\hat{Q}\hat{H}} : [0,1]\times[0,1] \rightarrow [0,1]$ that formulates the joint distribution $F_{\hat{Q}\ \hat{H}}$ of the pair $(\hat{Q}, \hat{H})$, with marginal distributions $F_{\hat{Q}}$ and $F_{\hat{H}}$, for all $(Q, H) \in R^2$, as:

$$F_{\hat{Q}\ \hat{H}}(Q,\ H) = C_{\hat{Q}\ \hat{H}}\left(F_{\hat{Q}}\ (Q), F_{\hat{H}}(H)\right) \tag{2}$$

The multivariate model is constructed by fitting suitable univariate laws on the marginals, and an appropriate copula on the observed pairs (Genest and Favre, 2007; Salvadori et al., 2007). Here, we use the method of Sadegh et al. (2018) which comprehensively analyzes the dependence structure of multiple drivers of flooding, and models them using copula functions to estimate return design values and their underlying uncertainties. This approach first selects a marginal distribution from 17 univariate distributions based on measures of goodness-of-fit including Akaike Information Criterion (AIC) and Bayesian Information Criterion (BIC), and then chooses a copula model from 26 copula functions. Copula model parameters are inferred through a Bayesian inference approach with Markov Chain Monte Carlo (Sadegh et al., 2018, 2017). The joint probability can refer to the exceedance of $\hat{Q}$ AND $\hat{H}$ or the exceedance of $\hat{Q}$ OR $\hat{H}$ (Salvadori et al., 2016), and a case can be made for the relevance of both to coastal flood hazard assessment. First of all, risk assessment should reflect the possibility that flooding is caused by either extreme river discharge or extreme ocean levels, which is consistent with the OR scenario. On the other hand, hydrodynamic modeling involves the simultaneous occurrence of an upstream discharge and downstream water level, consistent with the AND scenario.

Newport Bay data are used to illustrate this process. Fig. 3 presents the outcome of bivariate statistical analysis using both the OR and the AND hazard scenarios using the method of Sadegh et al. (2018). There is no statistically significant correlation between river flow and ocean water level at Newport Bay, but correlation was found between river flow and non-tidal residual (NTR) defined as the difference between TWL and the astronomical tide level. Hence, bivariate statistical analysis that takes correlation structure into account is presented here using river flow and NTR. Fig. 3 illustrates the similarities and differences between univariate and bivariate statistical analysis as well as the relative complexity introduced by the copula based AND and OR hazard scenarios. In particular, Fig. 3 shows plots of the marginal distributions of NTR (Fig. 3a) and river flow (Fig. 3c) representative of what has traditionally been used for univariate flood hazard assessment, while Fig. 3b shows the copula-based AND and OR hazard scenarios. The AND and OR hazard scenarios are shown as iso- return period curve for $T = 50$ year within a two-dimensional space whereby every point corresponds to a possible $(\hat{Q}_T, \hat{H}_T)$ pair for use in hydrodynamic modeling. Additionally, along each iso- return period curve, there is a point of maximum probability density which represents the most likely $(\hat{Q}_T, \hat{H}_T)$ pairs given the correlation structure. Note that the most likely $(\hat{Q}_T, \hat{H}_T)$ pair for the OR hazard scenario exceeds extreme values given by the marginal distributions, while the most likely $(\hat{Q}_T, \hat{H}_T)$ pair for the AND hazard scenario falls below the values given by the marginal distributions. This shows that the OR hazard scenario will lead to boundary forcing that is more conservative (meaning a more cautious approach to risk management perspective) than the AND hazard scenario.

Given theoretical characteristics of the OR iso-return period curves (Salvadori et al., 2016) boundary forcing associated with $(\hat{Q}_T, \hat{H}_T)$ pairs at the ends of the OR curve may far exceed values given by the marginal distributions for the same return period. This shows that the OR scenario creates seemingly unrealistic (highly conservative) hazard scenarios in areas of low probability density.

Hydrodynamic modeling of compound flood hazards for return period T is proposed based on four specific $(\hat{Q}_T, \hat{H}_T)$ pairs taken from bivariate statistical analysis as shown in Fig. 3:

(S1) A "Marginal Q" scenario defined by the T-year return period river discharge and a non-extreme water level downstream (typically taken as mean higher high water).
(S2) A "Marginal H" scenario defined by the T-year return period ocean water level and a non-extreme river flow (typically taken as the daily average flow).
(S3) An "AND" scenario based on the $(\hat{Q}_T, \hat{H}_T)$ pair with the highest probability density along the AND iso-return period curve.
(S4) An "OR" scenario based on the $(\hat{Q}_T, \hat{H}_T)$ pair with the highest probability density along the OR iso-return period curve.

FEMA (2015) presently recommends hydrodynamic modeling of S1 and S2 and estimation of $\eta_T(x)$ based on the maximum of the two. Hence, two additional scenarios (S3 and S4) are considered here as a way of leveraging bivariate statistical analysis.

2.3. Hydrodynamic modeling

Dynamic changes in water surface elevation within estuaries can be modeled with reasonable accuracy using shallow-water hydrodynamic models that assume a constant fluid density and a depth-averaged horizontal velocity (Sanders et al., 2010; FEMA, 2015, 2018). Estuaries involve the mixing of riverine and ocean water with different densities, and may be characterized by strong vertical density stratification that acts as a major control on the velocity distribution and transport (Geyer, 2010; Monismith, 2010). Consequently, three-dimensional models that account for variable density from salinity and temperature are often needed to estimate velocity distributions (Jay, 2010). However, the expression of density effects on surface water elevation is weak and can be neglected when predicting extreme water levels for the purpose of flood hazard modeling (Friedrichs, 2010). In this study, water levels are modeled by solving one-dimensional, constant density, steady-state shallow-water models (Chow, 2009) and two-dimensional, constant density, depth-averaged, shallow-water equations (Kim et al., 2015). When a model is set up for estuaries, tidal embayments, or tidal channels, the required boundary conditions correspond to a time series of river discharge at the upstream boundary, $Q(t)$, and a time series of water level, $H(t)$, at the downstream boundary. The upstream and downstream boundaries of the modeled spatial domain are generally placed adequately apart that compounding effects are avoided. This is not, however, always possible in practice because tide gauges may be located within estuaries. As an aside, we note that two-dimensional models require a spatial distribution of boundary forcing and in practice, hydrodynamic models include methods to distribute the total volumetric flow rate, $Q(t)$, across the inflow boundary while the water level, $H(t)$, is typically assumed to be uniform across the outflow boundary. Estuaries may also experience water level variability from internal forcing by winds and waves, and accounting for these effects is outside the scope of this study. However, the role of regional winds, waves, and atmospheric pressure on water levels is captured by this approach based on the measurement of water levels at the tide gauge used for bivariate flood hazard assessment.

2.3.1. 1D steady state modeling

One-dimensional (1D) steady state modeling of coastal flood hazards is useful as a first approximation of flood hazard levels along tidal channels and estuaries and can be done quickly with low computational effort. Application of 1D analysis at several sites is performed to study how differences in the selection process for $(\hat{Q}_T, \hat{H}_T)$ pairs can affect the estimation of flood hazard levels. Flood hazard levels are computed by solving the gradually varied flow equation under the assumption of a

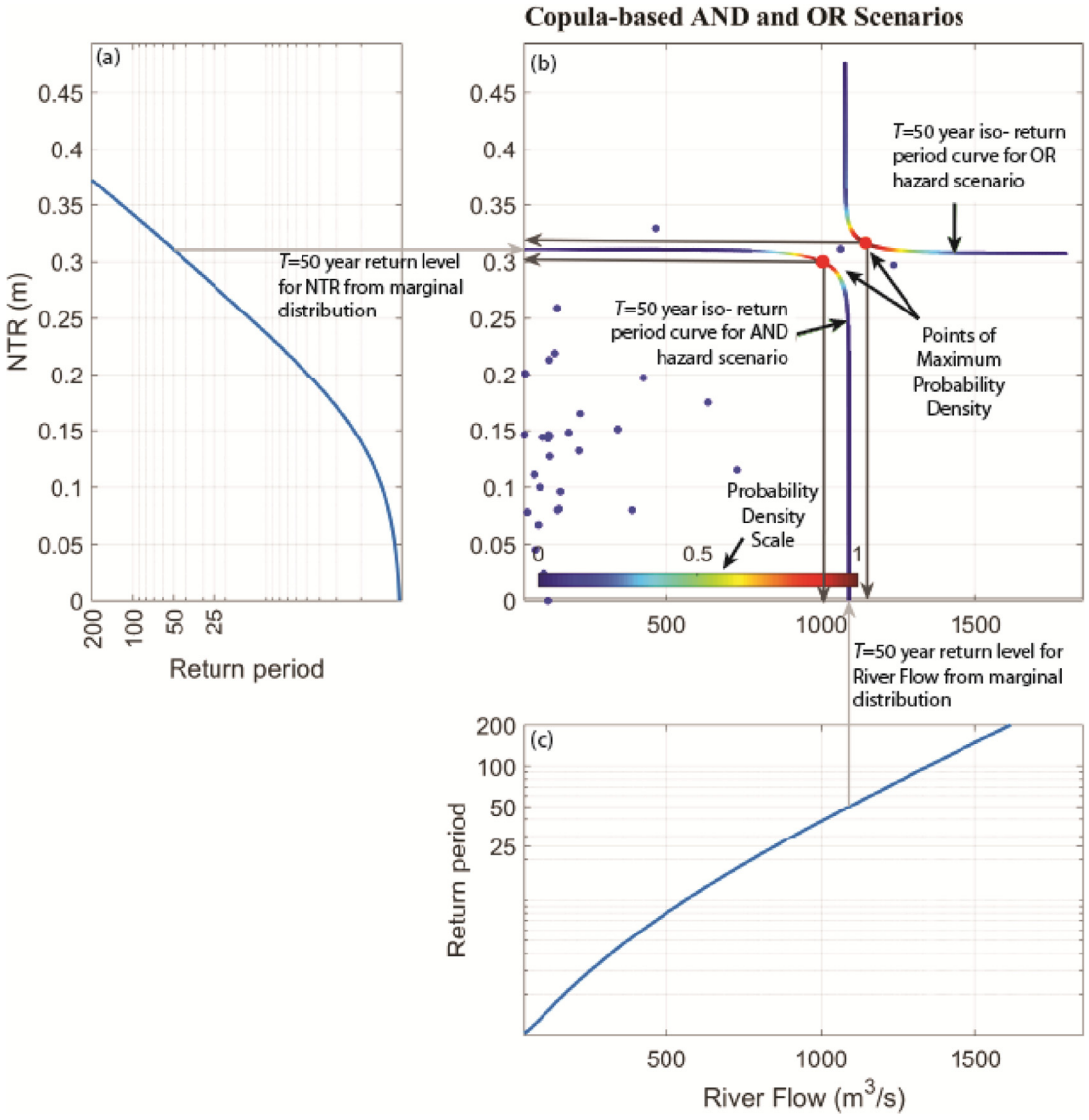

Fig. 3. Marginal probability distribution for (a) non-tidal residual (NTR) which is a surrogate for $\hat{H}$ and (c) River Flow $\hat{Q}$; (b) bivariate statistical analysis of $(\hat{Q}_T, \hat{H}_T)$ pairs based on copula-based AND and OR hazard scenarios. Two iso- return period curves corresponding to $T = 50$ year are shown. Note that ends of the copula-based scenario curves for return period T are aligned with the return level of the marginal distribution for return period T. Note also that along each $T = 50$ year curve, there is a point of maximum probability density which (due to correlation structure) represents the most likely $(\hat{Q}_T, \hat{H}_T)$ pairs. The most likely $(\hat{Q}_T, \hat{H}_T)$ pair for the OR hazard scenario exceeds extreme values given by the marginal distributions, while the most likely $(\hat{Q}_T, \hat{H}_T)$ pair for the AND hazard scenario falls below the values given by the marginal distributions.

rectangular channel with spatially variable Manning n_m, width w, and depth h as follows (Chow, 2009)

$$\frac{\mathrm{d}\,\eta}{\mathrm{d}x} = -\frac{S_f}{1 - Fr^2} \tag{3}$$

where x represents distance measured inland from the mouth of the estuary, $Fr = Q/(gh^3w^2)^{1/2}$ is the Froude Number and $S_f = (n_m\, Q/w)^2/\mathrm{h}^{10/3}$ represents the friction slope. Eq. (3) is integrated with geometrical data for each site, $n_m = 0.032\ m^{-1/3}$ s, the downstream water level boundary given by $\hat{H}$, and a river discharge given by $\hat{Q}$. Numerical integration is performed with the 4th/5th order Runge Kutta Scheme ode45 supported by Matlab (Mathworks, Natick, MA). We note that the relatively simple channel geometry and resistance approximation is used herein to examine the relative differences between profiles from Scenarios S1–S4, and not to estimate flood hazard along these rivers in an absolute sense. More detailed geometry and resistance modeling will change the absolute value of flood hazard heights, but have little impact on the relative difference between scenarios.

2.3.2. 2D unsteady modeling

Two-dimensional (2D) unsteady modeling is performed at one of the four sites, Newport Bay, to characterize limitations of the 1D steady state approximation and to study how the relative timing of the flood peak and high tide level can affect the flood hazard characterization. The 2D model BreZo (Begnudelli et al., 2008; Kim et al., 2015) is applied based on a previous validation at Newport Bay (Gallien et al., 2011, 2014). BreZo relies on an unstructured mesh of triangular elements with varying size to capture the Bay's topography and bathymetry. The model was originally setup to predict flood impacts in the urbanized portions of the Newport Bay (City of Newport Beach, California, 2008). It features a fine resolution mesh with 3 m average linear resolution cells across streets and land parcels, while across the upper Newport Bay the average linear cell resolution is approximately 15 m. The boundary conditions in BreZo are setup to specify the riverine discharge $\hat{Q}$ entering the upper Newport Bay at the outlet of the San Diego Creek, while water level $\hat{H}$ is specified along a boundary placed a short distance offshore of the embayment.

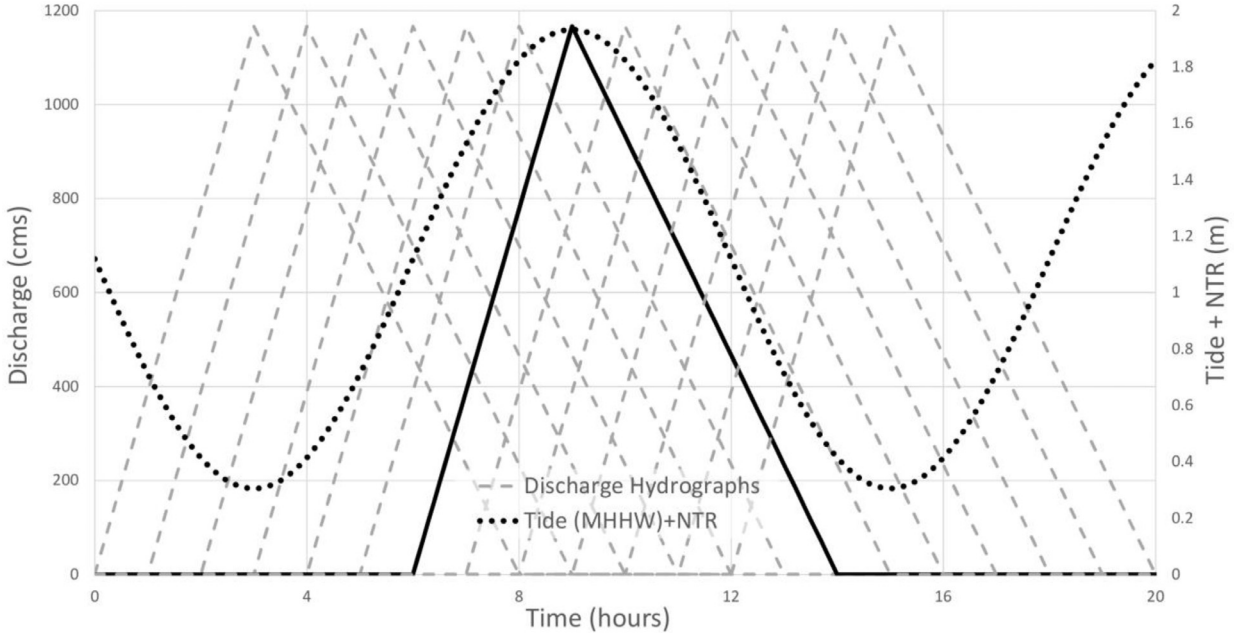

Fig. 4. Inflow into Newport Bay was modeled with a triangular hydrograph with a duration and time to rise specified based on historical average values, and the ocean water level was modeled with a sinusoidal function with a period of 12 h based on semidiurnal tides. The sensitivity of water level predictions to the time lag between peak river flow and high tide was examined with additional simulations involving forward and backwards time lags up to 6 h.

For unsteady analysis, riverine discharge entering Newport Bay was modeled with a triangular hydrograph with a peak value given by $\hat{Q}$ and a time of rise and total flood duration set to 3 and 8 h, respectively, based on analysis of instantaneous discharge measurements. Additionally, ocean water level changes were modeled using a sinusoidal function with a 12 h period (based on semidiurnal tides) such that the maximum ocean water level equals $\hat{H}$. These approximations followed preliminary modeling, which demonstrated that flood heights in the upper bay were much more sensitive to the magnitude of the peak flow than the duration of the event, within the range of observed values, and that high-water levels were not sensitive to the precise shape of the tidal forcing. We note that this may not be true in all systems, and thus these approximations are not presented as a generalization but rather as a reasonable simplification given specific site conditions.

Fig. 4 presents the sinusoidal ocean forcing and the triangular inflow hydrograph. To report the sensitivity of maximum water levels to the relative timing of the peak inflow and peak high tide, the "OR" Hazard Scenario was repeated using an inflow hydrograph that was shifted forward and backwater by as much as 6 h, as shown in Fig. 4.

All modeling results are expressed in metric units and referenced to the NAD83 State Plane horizontal coordinate system and NAVD88 vertical datum.

3. Results

3.1. Bivariate statistical analysis

Correlation analysis between $\hat{Q}$ and $\hat{H}$ defined by TWL revealed no statistical significance at these southern California sites due to relatively small storm surges compared to variability in high tide levels attributed to astronomical factors. However, correlation was found using NTR as a surrogate for $\hat{H}$ at three of the four sites considered: LAR, SAR and NB.

Kendall tau and Spearman rho correlation coefficients between variables $\hat{Q}$ and $\hat{H}$ (defined using NTR) are presented in Table 1 along with p-values. A p-value of less than 0.05 suggests a correlation at 5% significance level. Table 1 also shows the distribution functions that best describe the univariate distribution of river flow and NTR. Additionally, the JOE bivariate Copula function was found to best describe the correlation structure between $\hat{Q}$ and $\hat{H}$ in all sites.

Flood hazard levels $\hat{Q}$ and $\hat{H}$ for $T = 50$ year for Scenarios S1–S4 are presented in Table 2. Note that the "Marginal Q" scenarios all use a downstream water level corresponding to mean higher high water, and all of the "Marginal H" scenarios use a small (relative to the extreme flows) river discharge (~ average daily flow) taken as 10 m^3/s. These results show that the LAR has larger river discharge values than SAR and NB, yet somewhat surprisingly, NB has larger river discharge values than SAR despite a much smaller watershed area. This is attributed to control of runoff by dams. Also, note that the water level of the "Marginal H" scenario differs between the three sites despite all three relying on the Los Angeles Tide gauge. This is attributed to differences in the record length arising from joint probability analysis of tide gauge data and river gauge data.

3.2. 1D flood hazard analysis

1D steady state water surface profiles were computed for the 12 sets of $(\hat{Q}_T, \hat{H}_T)$ pairs presented in Table 2 corresponding to S1–S4 at LAR, SAR and NB and are presented in Fig. 5a, c, and e, respectively. Focusing first on the "Marginal H" and "Marginal Q" scenarios, these results shows that there is a transition in the dominant factor controlling flood hazard levels along the length of the system with H controlling flood hazards near the outlet and Q controlling flood hazards further inland. The length of oceanic control is relatively long for NB (~4 km) and LAR (~2 km) and relatively short SAR (~300 m). Water levels from the "AND" scenario are lower than the higher of the two marginal scenarios at inflow and outflow boundaries, but, higher within an interior region where the marginal profiles intersect. On the other hand, the "OR" scenario yields a water surface profile that is always above both marginal scenario profiles. Conceptually, these results show that the "OR" scenario represents a more conservative (i.e., cautious) representation of the spatially variable water surface profile associated with return period T than the "AND" scenario which is expected based on the magnitude of the boundary forcing (see Table 2).

FEMA (2015) guidance recommends mapping of flood hazard levels in tidally affected reaches based on the pointwise maximum of the

Table 1
Correlation coefficients between variables $\hat{Q}$ and $\hat{H}$.

Site	Kendall		Spearman		Pearson		Distribution	
	Correlation coefficient	*p*-value	Correlation coefficient	*p*-value	Correlation coefficient	*p*-value	Q	H
LAR	0.2616	0.0167	0.3880	0.0122	0.4666	0.0021	Rayleigh	Logistic
SAR	0.3357	0.0012	0.4907	0.0006	0.4303	0.0032	Nakagami	Logistic
NB	0.3229	0.0113	0.4478	0.0115	0.5659	0.0009	Inverse gaussian	Logistic

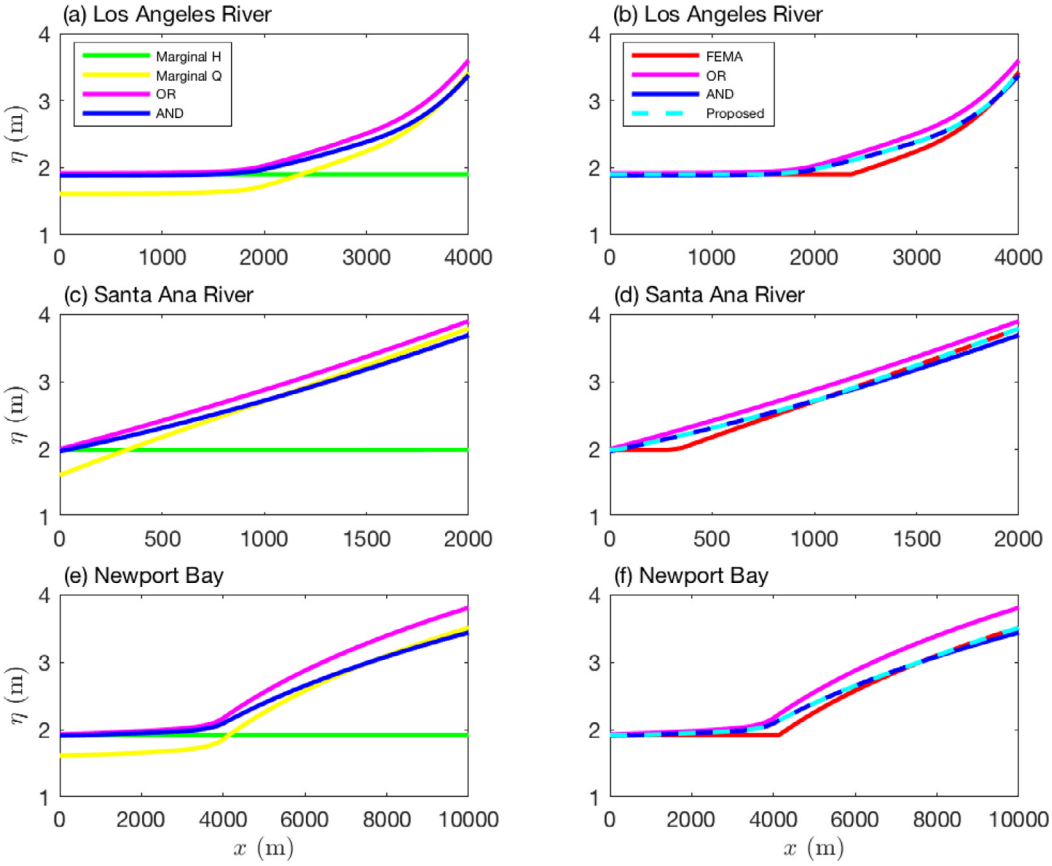

Fig. 5. Steady state water surface profiles versus distance from mouth, *x*, based on "Marginal H", "Marginal Q", "OR" and "AND" scenarios for (a) LAR, (c) SAR and (e) NB. Composite profiles based on the FEMA methodology and a proposed extension that considers the "Most Likely AND" scenario for (b) LAR, (d) SAR and (f) NB.

Table 2
Scenario S1–S4 values of the 50-year return period river discharge (m^3/s) and ocean level (m above NAVD88) resulting from bivariate analysis as shown in Fig. 3. Note that the AND and OR values correspond to maximum probability density (or likelihood).

Site	S1: Marginal Q		S2: Marginal H		S3: AND		S4: OR	
	$\hat{Q}$	$\hat{H}$	$\hat{Q}$	$\hat{H}$	$\hat{Q}$	$\hat{H}$	$\hat{Q}$	$\hat{H}$
LAR	2435	1.611	10	1.901	2295	1.882	2531	1.914
SAR	693	1.611	10	1.983	640	1.965	730	1.997
NB	1090	1.611	10	1.922	1005	1.911	1167	1.930

two marginal scenarios. This profile (labeled "FEMA") is presented in Fig. 5b, d, and f for LAR, SAR and NB, respectively, alongside the "AND", "OR", and a proposed composite profile based on the pointwise maximum of the "H Marginal", "Q Marginal" and "AND" hazard scenarios. At all three sites, the FEMA method underestimates the *T* year return period water level, compared to the "AND" scenario, within a region where the marginal water surface profiles intersect. Hence, the proposed composite profile is slightly higher than the FEMA method profile where there are physical compounding effects due to the interaction of river and oceanic influences on water levels; otherwise the proposed composite profile tracks the FEMA method profile.

3.3. 2D flood hazard analysis

Two-dimensional modeling of flood hazards in Newport Bay leads to spatially and temporally distributed water levels. Hence, flood hazards are mapped based on the point maximum water level attained over an unsteady simulation covering the rise and fall of a flood peak with magnitude $\hat{Q}$ and the rise and fall of an ocean tide of height $\hat{H}$. Results are presented first for the case of the temporal coincidence in the two peaks, and later the sensitivity of the results to the time lag between peaks is shown.

A comparison of extreme water level scenarios (S1–S4) along the main channel of Newport bay using 1D and 2D methods is shown in Fig. 6. For each scenario, the modeling method has little impact on water profiles in the lower bay ($x < 4000$ m) while differences are evident in upper bay ($x > 4000$ m) and attributed mainly to differences in the treatment of complex system topography/bathymetry. That is, the 1D model assumes a rectangular cross-sectional with a width and depth

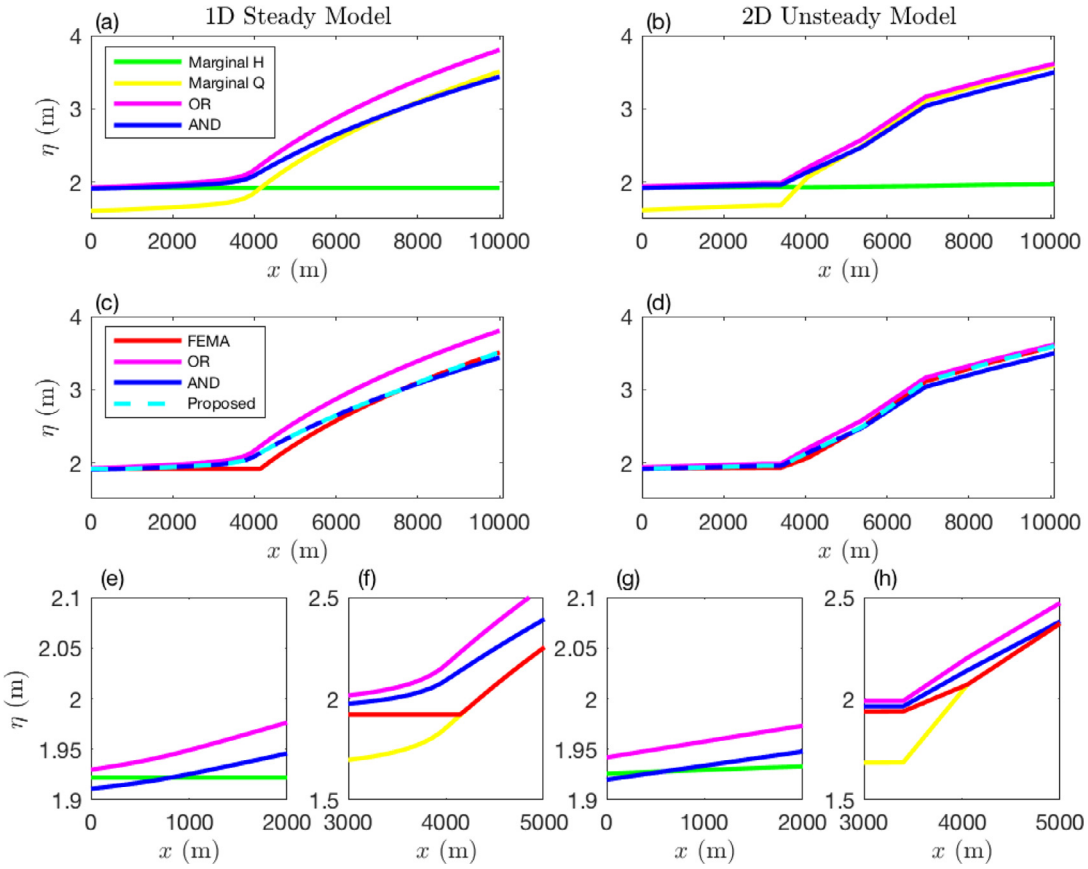

Fig. 6. NB flood hazard levels versus distance from mouth, x, based on 1D steady model (a, c, e, f) and 2D unsteady model (b, d, g, h). 2D results based on 5 points selected from along the main channel and linearly interpolated between points. Using both 1D and 2D approaches, the "AND" scenario predicts lower flood hazard levels compared to the maximum of the marginal profiles at the mouth ($x = 0$) and head ($x = 10{,}000$ m), and higher flood hazard levels near where the marginal profiles intersect ($x = 4000$ m).; the "OR" scenario predicts the highest water levels everywhere. Differences between 1D and 2D models attributed to unsteadiness and treatment of complex geometry.

based on the main channel, while the 2D model resolves both channel and floodplain/marsh topography allowing for greater conveyance at higher flood stages. Similar to the 1D model results presented earlier, the 2D results show that the "AND" scenario predicts lower flood hazard levels compared to the maximum of the marginal profiles at the mouth ($x = 0$) and head ($x = 10{,}000$ m), and higher flood hazard levels near where the marginal profiles intersect ($x = 4000$ m). Additionally, the "OR" scenario predicts the highest water levels everywhere. A magnified view of water surface profiles at the mouth is presented in Fig. 6e (1D) and 6 g (2D) and at $x = 4000$ m in Fig. 6f (1D) and 6 h (2D).

Fig. 6 also shows the FEMA (2015) composite profile and the proposed composite water surface profile, which takes the pointwise maximum of the marginal scenarios and the "AND" scenario. In this case, the 2D modeling predicts a smaller difference between composite profiles (~6 cm) than 1D modeling (~15 cm) and this is attributed mainly to the treatment of complex topography. Nevertheless, small height differences can be significant with respect to the delineation of flood hazard zones where floodplain topography is relatively flat. For example, a vertical height of 6 cm on a slope of 1/1000 implies a 60 m change in horizontal position which is larger than many land parcels in developed areas.

Fig. 7a shows the spatial distribution of the differences between water surface levels based on the FEMA method and the proposed method. The largest differences ($d\eta \geq 1$ cm) are found in the lower NB and are maximum at the constriction between upper and lower bay located at Pacific Coast Highway. Fig. 7a also shows differences in the western part of NB, off line from the main channel connecting San Diego Creek to the mouth of NB.

The effect of the relative timing of peak inflow and high tide to achieve maximum water surface elevations using the "OR" Hazard scenario was found to be relatively small compared to differences between hazard scenarios (i.e., AND vs. OR). Fig. 7b shows color contours of the difference in water surface elevations between the scenario where hydrograph peaks are matched in time (peak at time = 9 h in Fig. 4) and water surface elevations obtained by shifting the peaks in time to achieve maximum water level. In the uppermost section of the upper bay maximum water level is achieved by delaying peak river discharge by one hour (peak Q at hour 10 in Fig. 4), while in the lower bay maximum water level is achieved by advancing peak Q by one hour (peak Q at hour 8 in Fig. 4). The difference between water levels based on the timing of high tides vs peak flow was found to be less than 3 cm across the majority of the bay. This constitutes only about a third of the difference between the proposed composite profile and the FEMA (2015) composite profile. This result provides *a posteriori* validation of selecting Q and H as the basis for bivariate statistical analysis at this site as opposed to other system attributes such as the time lag between river flow and high tide.

4. Discussion

Multivariate statistical analysis is limited here to two variables (bivariate analysis) chosen to represent annual maximum river discharge and ocean level. Hazard scenarios beyond two variables are possible using copula-based methods, however expansion to higher dimensions can have drawbacks including uncertainty bounds so large that no conclusion may be drawn from its results (see Bevacqua et al. (2017) for

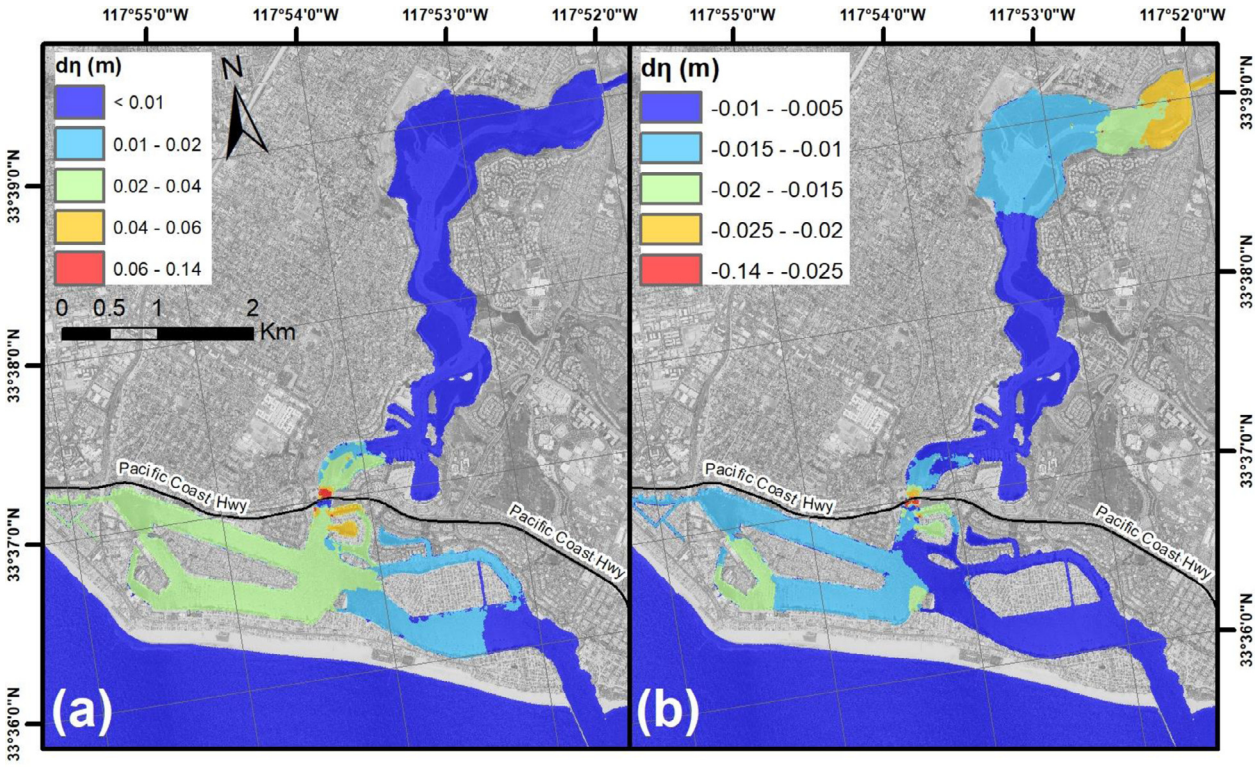

Fig. 7. Difference in water surface elevations between (a) the proposed composite profile and the FEMA composite profile, and (b) "OR Hazard" scenarios with coincident peaks at hour 9 vs scenarios with shifted peaks that achieve maximum water surface level.

example). For the sites considered, the importance of the randomness of annual maximum river discharge and ocean level (over other variables) justifies the formulation of the bivariate statistical analysis problem around these two variables. In systems where flood hazards are controlled by randomness in other factors such as waves or rainfall or even uncertain internal processes, a different approach would be needed. Examples of internal processes include the frictional interaction between streamflow and tidal levels (Kukulka and Jay, 2003a,b; Moftakhari et al., 2013, 2016). Applications at a broader set of sites are warranted to better understand the broader applicability of the proposed method of bivariate analysis for flood hazard assessment in tidal channels and estuaries.

Composite profiles derived from the pointwise maximum of water levels predicted by two or more hydrodynamic modeling scenarios offer a practical approach for delineating compound flood hazards in tidal channels and estuaries for a return period, T. Only a limited number of (relatively expensive) hydrodynamic model simulations need to be completed despite an infinite number of possible forcing scenarios based on bivariate statistical analysis. The most likely "AND" hazard scenario was identified as a promising candidate for extending FEMA (2015) guidance on flood hazard mapping in tidal channels and estuaries. That is, results here suggest that the FEMA (2015) method may underestimate the flood hazard level over an interior section of tidal reaches and estuaries where high water levels are sensitive to both riverine discharge and ocean levels. In NB, this section corresponds to the urbanized lower bay where exposure and vulnerability to flooding is highest. Moreover, an important implication is that extreme water levels may be higher at certain points within a system from combinations of river discharge and ocean heights that both fall below the return levels given by the marginal distribution (i.e., univariate analysis). On the other hand, the most likely "OR" hazard scenario results in boundary forcing that exceeds the return levels given by univariate analysis, and it produces water levels that are higher than the marginal scenarios and the "AND" hazard scenario. The "OR" hazard scenario could be useful when there is interest in using a single hydrodynamic modeling scenario to represent compound flood hazard levels and to avoid the need to compute composite profiles from multiple hydrodynamic modeling scenarios. Importantly, the "OR" hazard represents a more conservative interpretation of the T year return period hazard compared to traditional univariate assessment methods as well the "AND" hazard scenario.

This paper points to the possibility of a more robust framework for mapping coastal flood hazards in tidal channels in estuaries that takes advantage of recent advances in multivariate statistical modeling (e.g., Sadegh et al., 2018) and hydrodynamic coastal flood hazard mapping (e.g., Gallien et al. 2011; Luke et al., 2018) and is in line with the limited resources and past practices of flood hazard mapping (Burby 2001; FEMA 2015). In short, the method involves: (1) bivariate statistical analysis where correlations in extreme values exist, (2) selection of a limited number of $(\hat{Q}_T, \hat{H}_T)$ for return period T, (3) hydrodynamic modeling of the chosen pairs to produce extreme water levels, and (4) synthesis of the model results to provide a spatial distribution of water level associated with return period T. If this approach is taken to be more robust than existing methods (and more research will be needed at a broader set of sites to make this assessment), then the limited testing presented herein points to the existence of compound flood hazards that are presently underestimated by the existing FEMA method for tidal channels (FEMA, 2015). That is, at all three sites, there was a reach of the channel where the proposed composite profile accounting for the "AND" hazard scenario was higher than the composite profile accounting only for marginal scenarios as a result of physical compounding effects. Recent research has also shown that flood hazard zones in the U.S. are underestimated due to poor representation of pluvial flood hazards (e.g., Wing et al., 2017).

Finally, we note that the hydrodynamic modeling shown here for Newport Bay is for only a single return period to demonstrate the hybrid statistical-hydrodynamic framework. Assessment of flood hazard levels corresonding to other return periods follows the same approach.

5. Conclusions

A method of linking statistical analysis with hydrodynamic modeling to estimate spatially distributed compound flood hazard levels in tidal channels and estuaries is presented for cases where flood hazards are associated with both high river discharge (upstream forcing) and high ocean levels (downstream forcing). Bivariate statistical analysis is introduced to create combinations of river discharge and ocean levels suited for hydrodynamic modeling, and extreme water levels produced by hydrodynamic models are synthesized to create a composite water surface profile representative of return period, T. The method accounts for compound flood hazards in two ways. First, it accounts for statistical correlation between upstream and downstream forcing which represents one dimension of compound hazards. Secondly, hydrodynamic modeling accounts for physical compounding effects. Importantly, this work shows that water levels at interior points of a tidal channel or estuary resulting from the bivariate "AND" hazard scenario can be higher than water levels from marginal scenarios even though the boundary forcing is smaller than the corresponding marginal scenarios. This is attributed to physical compounding effects, i.e., nonlinear interactions between discharge and water level described by shallow-water wave theory. This work also shows that if a single scenario is needed to depict spatially distributed compound flood hazard levels, the bivariate "OR" hazard can be used and results here show that it provides a conservative assessment of the T year return period hazard.

Acknowledgments

This research was made possible by grants from the National Science Foundation Hazards-SEES Program (award DMS 1331611) and the National Oceanic and Atmospheric Administration Ecological Effects of Sea Level Rise Program (award NA16NOS4780206), who support is gratefully acknowledged.

References

Begnudelli, L., Sanders, B.F., Bradford, S.F., 2008. Adaptive Godunov-based model for flood simulation. J. Hydraul. Eng. 134, 714–725. https://doi.org/10.1061/(ASCE)0733-9429(2008)134:6(714).

Bevacqua, E., Maraun, D., Hobæk Haff, I., Widmann, M., Vrac, M., 2017. Multivariate statistical modelling of compound events via pair-copula constructions: analysis of floods in Ravenna (Italy). Hydrol. Earth Syst. Sci. 21 (6), 2701–2723.

Burby, R.J., 2001. Flood insurance and floodplain management: the US experience. Environ. Hazards 3, 111–122. https://doi.org/10.3763/ehaz.2001.0310.

Chow, V.T., 2009. Open-Channel Hydraulics. Blackburn Press, Caldwell, NJ.

City of Newport Beach, California, 2008. Vulnerability of the Newport Harbor Area to Flooding by Extreme Tides.

Coles, S.G., Heffernan, J., Tawn, J., 1999. Dependence measures for extreme value analyses. Extremes 2, 339–365. https://doi.org/10.1023/A:1009963131610.

Dasgupta, S., Laplante, B., Murray, S., Wheeler, D., 2011. Exposure of developing countries to sea-level rise and storm surges. Clim. Change 106, 567–579. https://doi.org/10.1007/s10584-010-9959-6.

FEMA, 2018. Guidelines and Standards for Flood Risk Analysis and Mapping [WWW Document]. https://www.fema.gov/guidelines-and-standards-flood-risk-analysis-and-mapping.

FEMA, 2015. Guidance for Flood Risk Analysis and Mapping; Combined Coastal and Riverine Floodplain (No. Guidance Document 32). FEMA.

Friedrichs, C.T., 2010. Barotropic tides in channelized estuaries. In: Valle-Levinson, A. (Ed.), Contemporary Issues in Estuarine Physics. Cambridge University Press, Cambridge, pp. 27–61. https://doi.org/10.1017/CBO9780511676567.004.

Gallien, T., Kalligeris, N., Delisle, M.-P., Tang, B.-X., Lucey, J., Winters, M., 2018. Coastal flood modeling challenges in defended urban backshores. Geosciences 8, 450. https://doi.org/10.3390/geosciences8120450.

Gallien, T.W., Sanders, B.F., Flick, R.E., 2014. Urban coastal flood prediction: integrating wave overtopping, flood defenses and drainage. Coast. Eng. 91, 18–28. https://doi.org/10.1016/j.coastaleng.2014.04.007.

Gallien, T.W., Schubert, J.E., Sanders, B.F., 2011. Predicting tidal flooding of urbanized embayments: a modeling framework and data requirements. Coast. Eng. 58, 567–577. https://doi.org/10.1016/j.coastaleng.2011.01.011.

Genest, C., Favre, A.-C., 2007. Everything you always wanted to know about copula modeling but were afraid to ask. J. Hydrol. Eng. 12, 347–368. https://doi.org/10.1061/(ASCE)1084-0699(2007)12:4(347).

Geyer, W.R., 2010. Estuarine salinity structure and circulation. In: Valle-Levinson, A. (Ed.), Contemporary Issues in Estuarine Physics. Cambridge University Press, Cambridge, pp. 12–26. https://doi.org/10.1017/CBO9780511676567.003.

Hallegatte, S., Green, C., Nicholls, R.J., Corfee-Morlot, J., 2013. Future flood losses in major coastal cities. Nat. Clim. Change 3, 802–806. https://doi.org/10.1038/nclimate1979.

Hanson, S., Nicholls, R., Ranger, N., Hallegatte, S., Corfee-Morlot, J., Herweijer, C., Chateau, J., 2011. A global ranking of port cities with high exposure to climate extremes. Clim. Change 104, 89–111. https://doi.org/10.1007/s10584-010-9977-4.

Hao, Z., Singh, V.P., 2016. Review of dependence modeling in hydrology and water resources. Prog. Phys. Geogr. 40, 549–578. https://doi.org/10.1177/0309133316632460.

Hawkes, P.J., 2006. Use of Joint Probability Methods in Flood Management: A Guide to Best Practice (R&D Technical Report No. FD2308/TR2). DEFRA.

Hawkes, P.J., Gouldby, B.P., Tawn, J.A., Owen, M.W., 2002. The joint probability of waves and water levels in coastal engineering design. J. Hydraul. Res. 40, 241–251. https://doi.org/10.1080/00221680209499940.

Heffernan, J.E., Tawn, J.A., 2004. A conditional approach for multivariate extreme values (with discussion). J. R. Stat. Soc. Ser. B Stat. Methodol. 66, 497–546. https://doi.org/10.1111/j.1467-9868.2004.02050.x.

Hillier, J.K., Macdonald, N., Leckebusch, G.C., Stavrinides, A., 2015. Interactions between apparently 'primary' weather-driven hazards and their cost. Environ. Res. Lett. 10 (10), 104003.

Hinkel, J., Lincke, D., Vafeidis, A.T., Perrette, M., Nicholls, R.J., Tol, R.S.J., Marzeion, B., Fettweis, X., Ionescu, C., Levermann, A., 2014. Coastal flood damage and adaptation costs under 21st century sea-level rise. Proc. Natl. Acad. Sci. 111, 3292–3297. https://doi.org/10.1073/pnas.1222469111.

Hinkel, J., Nicholls, R.J., Vafeidis, A.T., Tol, R.S.J., Avagianou, T., 2010. Assessing risk of and adaptation to sea-level rise in the European Union: an application of DIVA. Mitig. Adapt. Strateg. Glob. Change 15, 703–719. https://doi.org/10.1007/s11027-010-9237-y.

Hoitink, A.J.F., Jay, D.A., 2016. Tidal river dynamics: implications for deltas. Rev. Geophys. 54, 240–272. https://doi.org/10.1002/2015RG000507.

Jay, D.A., 2010. Estuarine variability. In: Valle-Levinson, A. (Ed.), Contemporary Issues in Estuarine Physics. Cambridge University Press, Cambridge, pp. 62–99. https://doi.org/10.1017/CBO9780511676567.005.

Kappes, M.S., Keiler, M., von Elverfeldt, K., Glade, T., 2012. Challenges of analyzing multi-hazard risk: a review. Nat. Hazards 64 (2), 1925–1958.

Kennish, M.J. (Ed.), 2004. Estuarine research, monitoring, and resource protection, Marine Science Series. CRC Press, Boca Raton, Fla.

Kim, B., Sanders, B.F., Famiglietti, J.S., Guinot, V., 2015. Urban flood modeling with porous shallow-water equations: a case study of model errors in the presence of anisotropic porosity. J. Hydrol. 523, 680–692. https://doi.org/10.1016/j.jhydrol.2015.01.059.

Kukulka, T., Jay, D.A., 2003a. Impacts of Columbia River discharge on salmonid habitat: 1. A nonstationary fluvial tide model. J. Geophys. Res. 108.

Kukulka, T., Jay, D.A., 2003b. Impacts of Columbia River discharge on salmonid habitat: 2. Changes in shallow-water habitat. J. Geophys. Res. 108.

Lanzoni, S., Seminara, G., 1998. On tide propagation in convergent estuaries. J. Geophys. Res. Oceans 103, 30793–30812. https://doi.org/10.1029/1998JC900015.

Leonard, M., Westra, S., Phatak, A., Lambert, M., van den Hurk, B., McInnes, K., Risbey, J., Schuster, S., Jakob, D., Stafford-Smith, M., 2014. A compound event framework for understanding extreme impacts. Wiley Interdiscip. Rev. Clim. Change 5, 113–128. https://doi.org/10.1002/wcc.252.

Luke, A., Sanders, B.F., Goodrich, K.A., Feldman, D.L., Boudreau, D., Eguiarte, A., Serrano, K., Reyes, A., Schubert, J.E., AghaKouchak, A., Basolo, V., 2018. Going beyond the flood insurance rate map: insights from flood hazard map co-production. Nat. Hazards Earth Syst. Sci. 18 (4), 1097–1120.

Moftakhari, H.R., Jay, D.A., Talke, S.A., 2016. Estimating river discharge using multiple-tide gauges distributed along a channel. J. Geophys. Res. Oceans 121, 2078–2097. https://doi.org/10.1002/2015JC010983.

Moftakhari, H.R., Jay, D.A., Talke, S.A., Kukulka, T., Bromirski, P.D., 2013. A novel approach to flow estimation in tidal rivers. Water Resour. Res. 49, 4817–4832. https://doi.org/10.1002/wrcr.20363.

Moftakhari, G., Salvadori, AghaKouchak, A., Sanders, B.F., Matthew, R.A., 2017. Compounding effects of sea level rise and fluvial flooding. Proc. Natl. Acad. Sci. 114, 9785–9790. https://doi.org/10.1073/pnas.1620325114.

Monismith, S.G., 2010. Mixing in estuaries. In: Valle-Levinson, A. (Ed.), Contemporary Issues in Estuarine Physics. Cambridge University Press, Cambridge, pp. 145–185. https://doi.org/10.1017/CBO9780511676567.008.

Neal, J., Keef, C., Bates, P., Beven, K., Leedal, D., 2013. Probabilistic flood risk mapping including spatial dependence. Hydrol. Process. 27, 1349–1363. https://doi.org/10.1002/hyp.9572.

Purvis, M.J., Bates, P.D., Hayes, C.M., 2008. A probabilistic methodology to estimate future coastal flood risk due to sea level rise. Coast. Eng. 55, 1062–1073. https://doi.org/10.1016/j.coastaleng.2008.04.008.

Ross, D.A., 1995. Introduction to Oceanography. HarperCollinsCollegePublishers, New York, NY.

Sadegh, M., Moftakhari, H., Gupta, H.V., Ragno, E., Mazdiyasni, O., Sanders, B., Matthew, R., AghaKouchak, A., 2018. Multi-hazard scenarios for analysis of compound extreme events. Geophys. Res. Lett.. https://doi.org/10.1029/2018GL077317.

Sadegh, M., Ragno, E., AghaKouchak, A., 2017. Multivariate Copula Analysis Toolbox (MvCAT): describing dependence and underlying uncertainty using a Bayesian framework: MvCAT. Water Resour. Res. 53, 5166–5183. https://doi.org/10.1002/2016WR020242.

Salvadori, G., De Michele, C., Kottegoda, N., Rosso, R., 2007. Extremes in nature: an approach using copulas. Water Science and Technology Library. Springer, Dordrecht.

Salvadori, G., Durante, F., De Michele, C., Bernardi, M., Petrella, L., 2016. A multivariate Copula-based framework for dealing with Hazard Scenarios and Failure Probabilities. Water Resour. Res. 52, 3701–3721. https://doi.org/10.1002/2015WR017225.

Salvadori, G., Durante, F., Tomasicchio, G.R., D'Alessandro, F., 2015. Practical guidelines for the multivariate assessment of the structural risk in coastal and off-shore engineering. Coast. Eng. 95, 77–83. https://doi.org/10.1016/j.coastaleng.2014.09.007.

Sanders, B.F., 2017. Hydrodynamic modeling of urban flood flows and disaster risk reduction. Natural Hazard Science, Oxford Research Encyclopedias.

Sanders, B.F., Schubert, J.E., Detwiler, R.L., 2010. ParBreZo: a parallel, unstructured grid, Godunov-type, shallow-water code for high-resolution flood inundation modeling at the regional scale. Adv. Water Resour. 33, 1456–1467. https://doi.org/10.1016/j.advwatres.2010.07.007.

Sayers, P., Yuanyuan, L., Galloway, G., Penning-Rowsell, E., Fuxin, S., Kang, W., Yiwei, C., Le Quesne, T. (Eds.), 2013. Flood Risks Management: A Strategic Approach. Asian Development Bank, Mandaluyong City, Metro Manila, Philippines.

Scawthorn, C., Blais, N., Seligson, H., Tate, E., Mifflin, E., Thomas, W., Murphy, J., Jones, C., 2006. HAZUS-MH flood loss estimation methodology. I: overview and flood hazard characterization. Nat. Hazards Rev. 7, 60–71. https://doi.org/10.1061/(ASCE)1527-6988(2006)7:2(60).

Sklar, A., 1959. Fonctions de répartition à n dimensions et leurs marges. Publ Inst Stat. Univ Paris 8, 229–231.

Torresan, S., Critto, A., Rizzi, J., Marcomini, A., 2012. Assessment of coastal vulnerability to climate change hazards at the regional scale: the case study of the North Adriatic Sea. Nat. Hazards Earth Syst. Sci. 12, 2347–2368. https://doi.org/10.5194/nhess-12-2347-2012.

Ward, P.J., Couasnon, A., Eilander, D., Haigh, I.D., Hendry, A., Muis, S., Veldkamp, T.I.E., Winsemius, H.C., Wahl, T., 2018. Dependence between high sea-level and high river discharge increases flood hazard in global deltas and estuaries. Environ. Res. Lett. 13, 084012. https://doi.org/10.1088/1748-9326/aad400.

Wing, O.E., Bates, P.D., Sampson, C.C., Smith, A.M., Johnson, K.A., Erickson, T.A., 2017. Validation of a 30 m resolution flood hazard model of the conterminous United States. Water Resour. Res. 53 (9), 7968–7986.

Zheng, F., Leonard, M., Westra, S., 2015. Application of the design variable method to estimate coastal flood risk: design variable method to estimate flood risk. J. Flood Risk Manag. 1–13. https://doi.org/10.1111/jfr3.12180.

Zscheischler, J., Westra, S., van den Hurk, B.J.J.M., Seneviratne, S.I., Ward, P.J., Pitman, A., AghaKouchak, A., Bresch, D.N., Leonard, M., Wahl, T., Zhang, X., 2018. Future climate risk from compound events. Nat. Clim. Change. https://doi.org/10.1038/s41558-018-0156-3.